Evaluating the contribution of intermittent generation to power system adequacy at different demand levels

Esteban Gil
and Ignacio Aravena
Departamento de Ingeniería Eléctrica
Universidad Técnica Federico Santa María
Valparaíso, Chile

***Abstract*—This paper discusses the contribution of intermittent generation sources to power system adequacy for the Chilean Northern Interconnected System (SING) at different demand levels. Curves showing the system risk for different levels of demand are obtained using a Monte Carlo simulation approach that performs unit commitment and economic load dispatch, considering randomly generated outages and randomly selected synthetic wind and solar generation profiles created using a semi-parametric model. The simulation results are then used to estimate the probability of having energy not served for different demand levels. These curves can then be used to gain a better understanding of the contribution to adequacy of intermittent generators such as wind and solar (CPV and CSP), and the impact that thermal storage in CSP plants can make to improve their capacity value.**

***Index Terms*—Intermittent generation, power system adequacy, capacity value, wind power generation, solar power generation.**

I. Introduction

As penetration of non-conventional renewable energy (NCRE) grows, also grows the concern about the ability of the system to deliver a continuous supply of electricity despite the intermittency of the wind and solar resources. Thus, asking for the impact that intermittent generation resources such as wind and solar will have in power system reliability becomes relevant. The North American Electric Reliability Corporation (NERC) breaks down power system reliability in terms of both security and adequacy [1]. While security refers to the ability of the bulk power system to withstand and recover from sudden, unexpected disturbances, adequacy refers to having sufficient resources to supply the demand, taking into account unexpected outages of generators or transmission lines and possible constraints on the primary energy resource (problems on the fossil fuel chain of supply, dry spells, lack of wind). System adequacy is achieved by maintaining reserve capacity (especially during peak hours) to cover possible fluctuations in generation and demand and the risk of unexpected transmission or generation outages.

This work was supported in part by the Chilean National Commission for Scientific and Technological Research (CONICYT) under grant Fondecyt 11110502.

Generators with different operational characteristics will contribute differently to power system adequacy, contribution usually measured by their capacity value. Although the theory to determine the capacity value of conventional generation is well developed and the *Effective Load Carrying Capability* (ELCC) approach [2] has been in use for decades, during the last decade there has been a great deal of interest in determining the capacity value of intermittent generators [3]–[8], as the energy resource (wind speed or solar irradiation) is not always available and the conventional methods can not be applied without special considerations. The capacity value of intermittent generation sources depends on the correlation between the system risk and generation output. For example, a generating unit with higher output during high risk periods should be assigned a higher capacity value than a unit with the same capacity factor but available more during periods of low system risk.

This paper presents the results of a study to determine the contribution of wind and solar generators to power system adequacy in the Chilean Northern Interconnected System (*Sistema Interconectado del Norte Grande*, SING). Although the wind and solar energy potential in the SING remains mostly unexploited, its location in the Atacama desert (the driest desert in the world, with nearly non-existent cloud cover) suggests that there is an enormous but yet untapped potential for incorporating solar power into the generation mix. In order to gain an understanding of the specific contribution of intermittent generators to power system adequacy (usually measured by the capacity value), we explore the system risk for different levels of demand with and without some specific wind and solar generation projects.

This paper is structured as follows: Section II discusses how the system risk increases with the demand and presents the methodology used for evaluating the system risk in the SING. Section III describes the SING and the process of obtaining synthetic wind and solar data to use in the Monte Carlo scheme. Section IV presents the simulation results, and discusses the adequacy contribution of wind and solar generation. This section also discusses how heat storage may increase the adequacy contribution of CSP plants by displacing their generation to the peak hours. Finally, Section V presents the conclusions of the study.

II. System adequacy at different demand levels

The Loss of Load Probability (LOLP) is one of the most widely used metrics for power system adequacy. The LOLP is used in the resource adequacy arena by calculating the probability that system demand will exceed available generator capacity. Thus, in a system with no transmission constraints and with no time-coupling constraints (min up- and down-times, storage, generation ramps, among others) and independent failure modes, the LOLP can be calculated by doing convolution of the discrete probability distributions of the available capacity C_i of individual generators, as equations (1)-(3) show.

$$C_i = \begin{cases} 0 & p = \mathrm{FOR}_i \\ C_i^{\max} & p = 1 - \mathrm{FOR}_i \end{cases} \quad (1)$$

$$C_{\mathrm{sys}} = \sum_{i \in I} C_i \sim (C_1 * C_2 \ldots C_i \ldots C_{N-1} * C_N) \quad (2)$$

$$\mathrm{LOLP} = \mathbb{P}[D_{\mathrm{sys}} > C_{\mathrm{sys}}] \quad (3)$$

As the demand grows and the capacity reserve margin of a system tightens, the system risk increases as there will be fewer generating units available to balance demand and supply, and there will be more generating units that can suffer a forced outage and cause a loss-of-load event in the system. LOLP increases exponentially with the demand, and then converges to one as the demand exceeds the installed capacity of the system [9]. However, traditionally LOLP calculations do not consider aspects such as transmission constraints and losses, time-coupling constraints, energy-constrained generation, energy storage, pumping hydro, and/or demand response. Thus, when interested in evaluating the system risk considering operational issues, simulation techniques such as Monte Carlo methods are required [10], [11].

In this paper we use a stochastic production cost model with detailed DC power flow and unit commitment to measure the system risk, by calculating the probability that there would be energy not served happening anywhere in the system. In order to avoid confusion with the traditional definition of LOLP, we will be calling our metric Probability of Energy not Served (PENS). Although PENS is somehow similar to LOLP, LOLP calculations normally only consider generation capacity instead of generator energy output and usually do not include operational, energy, or transmission constraints.

Fig. 1 shows PENS and demand data pairs for the system obtained using the Monte Carlo simulation described in Section III. We can observe that despite the noise introduced by modeling detailed transmission and unit commitment the curve still shows an approximately exponential growth pattern. In order to obtain a less noisy curve we aggregate the energy not served instances for certain blocks of demand. This aggregation has the added advantage that it provides a greater number of samples for each demand level and decreases uncertainty on the estimate.

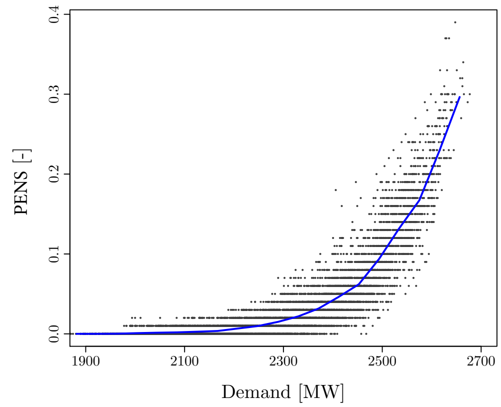

Fig. 1. Aggregation for the *No NCRE* case

III. Methodology

The objective of the modeling is to evaluate how intermittent generators such as wind and solar contribute to power system adequacy. In order to evaluate the system risk (as measured by the PENS) under different operating conditions (load, resource availability, and forced outages), a Monte Carlo based approach was implemented, based on a previous model presented in [12]. The algorithm runs market simulations for a whole year considering different stochastic samples, performing unit commitment and economic load dispatch for each sample. These random samples consist of: (1) randomly generated outage patterns for the different generators, obtained from their respective forced outage rates (FOR) and mean times to repair (MTTR), and (2) randomly generated selected wind and solar generation patterns, obtained as described in Section IV.

The market simulations were conducted using PLEXOS. PLEXOS is a production cost model capable of optimizing unit commitment and economic load dispatch. PLEXOS co-optimizes thermal, hydro, and ancillary services using Mixed Integer Linear Programming (MILP) and is able to perform Monte Carlo simulations [13]. Once PLEXOS formulates the mathematical program, it is solved using Xpress [14].

The simulation scheme solves a detailed hourly unit commitment using a forecast of demand and wind and solar power for the following day, and then fixes the unit commitment decisions for slow thermal generators. Then, Monte Carlo simulation is applied to the economic load dispatch. The Monte Carlo sampling is done to randomly determine forced outage patterns for each conventional generator and transmission line and to randomly select wind and solar power simulated patterns such that correlation between load and the intermittent generation is preserved. From the simulation results, the Energy-Not-Served (ENS) instances are counted for each demand level and the probability that there would be energy not served (PENS) is calculated. This method was applied to the SING to obtain a family of PENS-versus-demand curves that can be used to evaluate the contribution

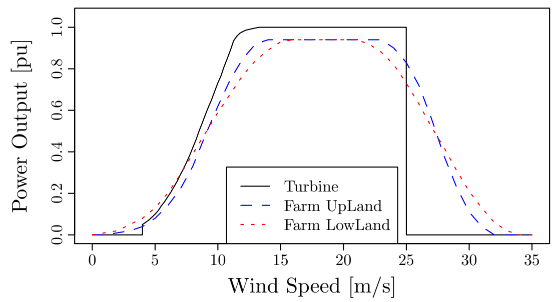

Fig. 2. Wind speed versus power curves for 2MW wind turbines in wind farms

of wind, concentrated photovoltaic (CPV), and concentrated solar power (CSP) generators to power system adequacy, as results in section V will show.

IV. Test System

A. SING characteristics

The SING is a system supplying mainly industrial load (about 90%) with 3.7 GW installed generation capacity in 2012. Electric energy supply comes mainly from coal-fired units (69.2% of total generation in 2011), some newer combined-cycle and open-cycle gas-fired units (25.8%), some fuel-oil and diesel peaking plants (3.9%), and a small amount of hydro generation (0.5%). The CDEC-SING, the SING independent system operator (ISO), provides on their website PLEXOS databases of their system containing detailed production and network data. These databases were adapted for the purposes of this work and the outputs of the simulations were benchmarked against actual system outputs to check for correctness and consistency. The SING market was simulated for the year 2015 based on National Energy Commission projections. In order to obtain a better estimation of the top of the PENS-versus-demand curve, we used a high demand scenario.

B. Wind and solar data

Two locations for wind farms and three locations for solar generators were considered in the study. Wind data was obtained from wind monitoring stations installed by the Chilean Department of Energy [15]. The first station (*Escondida*) is located in the lowlands close to the shore near *Antofagasta*, while the second one (*Estanque de Agua*) is located uplands near *Calama*. The datasets contain wind speed measurements taken at a height of 20 and 80 meters every 10 minutes from 2009 to 2011. Solar data was obtained from monitoring stations in *San Pedro de Atacama*, *Pozo Almonte*, and *Crucero*.

C. Creation of synthetic wind generation data

As the speed in different turbines in a wind farm is never the same, we used wind farm curves from [16], [17] to make the transformation from wind speed to power. Curves for lowland and upland wind farms are illustrated in fig. 2.

In the generation profiles two types of seasonal components were observed: one with a 24-hour period related to

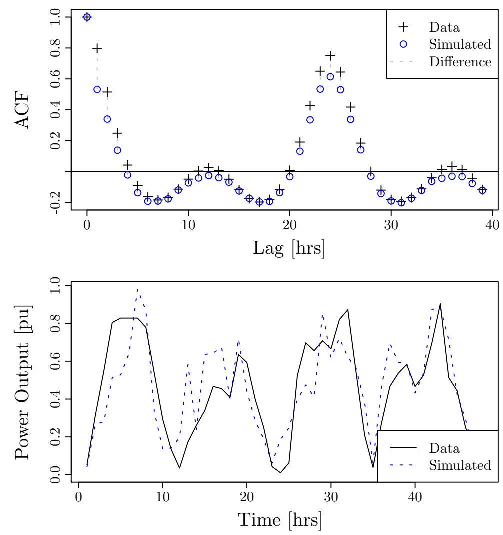

Fig. 3. Autocorrelation and 48-hour sample for original and synthetic data

temperature changes between day and night, and another one caused by seasonal changes. In order to run the Monte Carlo scheme we needed to create synthetic wind generation series. To preserve the observed seasonal components in a parametric model, too many parameters would have been needed, so we opted instead for a semi-parametric model that considered a non-parametric model of the seasonal components and a parametric model of the errors.

The model for extracting the seasonal patterns is based on the LOESS method, used as a low-pass filter. The yearly and daily seasonal components were extracted using a 30-day and a 1-day window for the low-pass filter, respectively, minus an error whose distribution can be approximated by a normal distribution. Then, new random errors are calculated from truncated normal distributions. They are truncated before generating the random errors, securing in this way that the synthetic series remains in the interval $(0,P_{\max})$. This approach is different to calculating the errors (or simulating the series) and then truncating the values, in which case we would be assigning a probability value to the limits and having a mixed discrete-continuous distribution for the innovations.

The results for the synthetic wind data presented in Figure 3 show that in general the autocorrelation of the original series is preserved. Similarly, the synthetic data preserve the seasonal patterns of the original series and are different of the original data, as the chart comparing 48 hours of the original and synthetic data series show.

The described methodology was contrasted against regressions using SARIMA models (simulated with errors from the truncated normal distributions mentioned above), and we obtained similar results in terms of the representation of the original profile, variation among synthetic data, and variation against the original data. However, the SARIMA results were worst in terms of capturing the autocorrelation of the process. Also, simulation of the SARIMA process with truncated errors was considerably slower than the LOESS-based model.

D. Creation of synthetic solar generation data

The procedure for generating synthetic solar generation data was simpler than in the wind case, as solar irradiation in the Atacama desert shows little variation from day to day (see boxplot in fig. 7), with most of the variability concentrating in the first and last hours of sun of each day (as the seasons change). Furthermore, solar irradiation shows little variation from one location to the other. Thus, to generate the synthetic solar generation datasets for each day we just used the solar irradiation data for a few days before and after each date.

V. Simulation results

A. Contribution to adequacy of wind farms

Using the Monte Carlo method described in Section III and the wind generation profiles obtained as described in Section IV-C, we simulated the system considering the following cases:

- Wind Interior: 400 MW wind farm using the *Wind Interior* synthetic profiles
- Wind Coast: 400 MW wind farm using the *Wind Coast* synthetic profiles
- Wind Coast-Interior: 2x200 MW wind farms, one using the *Wind Interior* profiles and the other using the *Wind Coast* profiles

Fig. 4 compares a boxplot of both wind farms' wind generation profiles (the box indicates the 25, 50 and 75 percentiles) against the percentage of ENS instances at different times of the day. The percentage of ENS instances for each hour is calculated with respect to the total ENS instances for the *No NCRE* case. We can suspect that despite *Wind Interior* having a higher capacity factor than *Wind Coast* (49% versus 38%), *Wind Coast* makes a greater contribution to improving system adequacy during the periods of high risk. This is confirmed by Fig. 5, showing system risk curves with and without the wind farms. As most of the risk concentrates in the periods of higher load, it is reasonable to think that *Wind Coast* should have a higher capacity value than *Wind Interior*, despite contributing less total energy to the system.

For the 3 cases studied, the system risk is reduced once the wind farms are added. This was to be expected, as we are adding more supply to the system and therefore improving its adequacy. But we can also observe that the adequacy contribution of the wind farms varies for different levels of demand/risk.

B. Contribution to adequacy of CPV

We obtained curves for 400 MW CPV generators in three different locations, but could not observe any meaningful differences between them. Fig. 7 compares a boxplot of the *San Pedro de Atacama* generation profiles against the percentage of ENS instances at different times of the day. As most of the system risk concentrates in the periods after sunset, solar CPV contribution during high-risk periods is relatively small, as fig. 6 confirms. This suggests that if the solar plant could

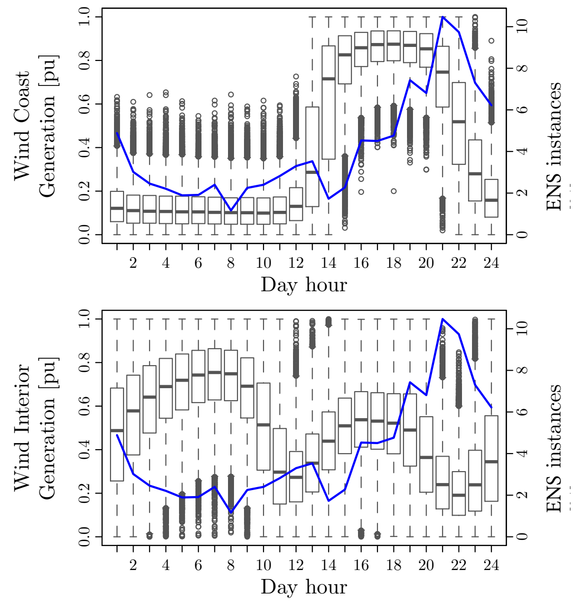

Fig. 4. Wind generation boxplot and percentage of ENS instances per hour

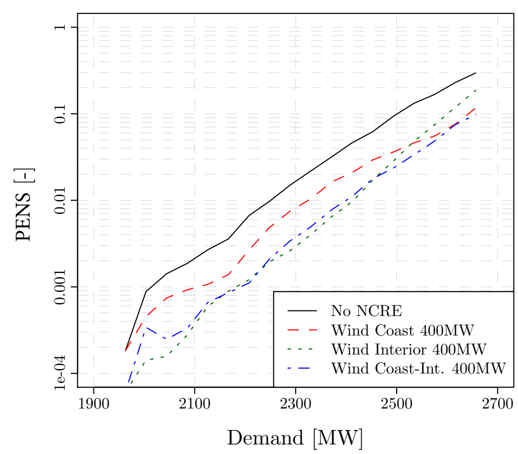

Fig. 5. Contribution to adequacy of wind farms

storage some of the energy for a few hours, it could make a greater contribution to power system adequacy.

C. Contribution to adequacy of CSP with and without storage

Concentrated solar-thermal technology has the option of using molten salt tanks to storage energy in the form of heat for use at a later time. In this way, CSP plants can displace its generation to hours with a higher price so as to increase their revenue. As the high-price hours generally coincide with the hours of high demand/risk, heat storage capability in CSP plants contribute to adequacy when it is more needed, that is, during the periods concentrating most of the risk. Thus, storage can increase their contribution to power system adequacy and therefore their capacity value.

Fig. 8 shows simulation results for a 200 MW CSP plant in *San Pedro de Atacama* with different levels of storage. It is easy to observe that the contribution of the storage to power

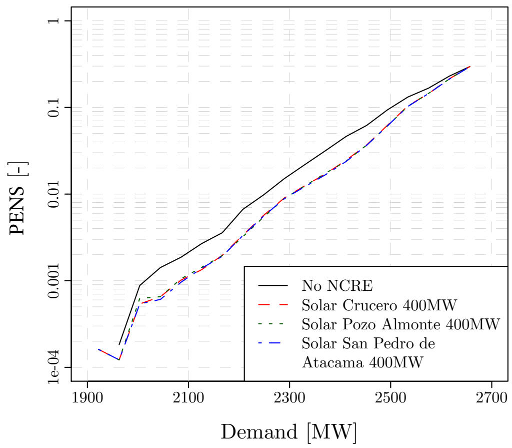

Fig. 6. Contribution to adequacy of CPV

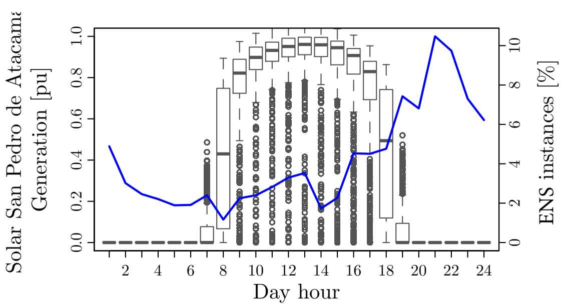

Fig. 7. Solar generation boxplot and percentage of ENS instances per hour

system adequacy happens mostly during high-risk periods. As the heat storage capacity increases, the contribution to adequacy also increases. Beyond 600MWh of storage (3 hours at maximum capacity for the 200 MW plant) there is no further reduction in the system risk. This can be explained by comparing the ENS instances per hour versus boxplots of the solar generation (without storage) per hour, as shown in Fig. 7.

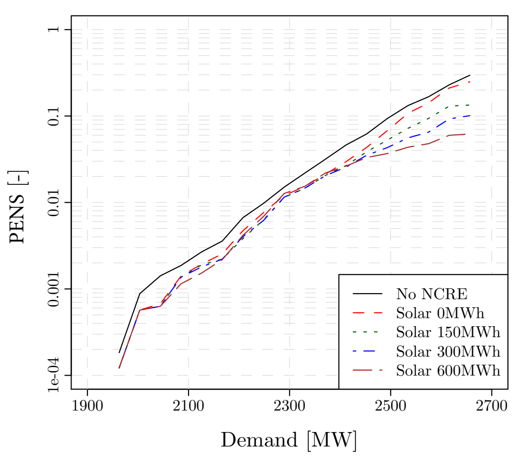

Fig. 8. Contribution to adequacy of CSP with different heat storage capacities

VI. Conclusions

This paper presented a Monte Carlo based approach to evaluate the contribution of wind and solar generators to power system adequacy, through the analysis of the system risk at different demand levels with and without the generators. The use of PENS-versus-demand curves allowed us to gain a better understanding of how each specific intermittent generator source contributes to risk reduction at different levels of demand. We could also appreciate how by adding storage capacity we can displace intermittent generation so that the peaks of the generation and the peak of the load coincide, in order to achieve a larger reduction of the risk during high-risk periods.

References

[1] NERC Board of Trustees, "Glossary of Terms Used in NERC Reliability Standards," NERC, Tech. Rep., dec. 2012.

[2] L. Garver, "Effective load carrying capability of generating units," *IEEE Transactions on Power Apparatus and Systems*, vol. PAS-85, no. 8, pp. 910–919, aug. 1966.

[3] M. Milligan and K. Porter, "The capacity value of wind in the united states: Methods and implementation," *The Electricity Journal*, vol. 19, no. 2, pp. 91–99, mar. 2006.

[4] C. D'Annunzio and S. Santoso, "Analysis of a wind farm's capacity value using a non-iterative method," in *IEEE Power and Energy Society General Meeting*, july 2008.

[5] M. Milligan and K. Porter, "Determining the capacity value of wind: An updated survey of methods and implementation," in *Wind Power Conference 2008*, Houston, Texas, june 2008.

[6] B. Hasche, A. Keane, and M. O'Malley, "Capacity value of wind power, calculation, and data requirements: the irish power system case," *IEEE Transactions on Power Systems*, vol. 26, no. 1, pp. 420–430, feb. 2011.

[7] M. Milligan, "Methods to model and calculate capacity contributions of variable generation for resource adequacy planning (ivgtf1-2): Additional discussion," presentation to NERC Loss of Load Expectation Working Group, Atlanta jan. 20, 2011.

[8] L. Soder and M. Amelin, "A review of different methodologies used for calculation of wind power capacity credit," in *IEEE Power and Energy Society General Meeting*, july 2008.

[9] E. Gil and I. Aravena, "A LOLP-based method to evaluate the contribution of wind generation to power system adequacy," in *Proc. of Fourth International Renewable Energy Congress (IREC2012)*, Sousse, Tunisia, dec. 2012, pp. 125–131.

[10] J. S. Bob Cummings, Mark Lauby, "Justification for a nerc resource adequacy assessment model: A nerc staff white paper," NERC, Tech. Rep., jul. 2007.

[11] J. Fazio, "A probabilistic method to assess power supply adequacy for the pacific northwest," Pacific Northwest Resource Adequacy Forum, Tech. Rep., oct. 2011.

[12] E. Gil, "Evaluating the impact of wind power uncertainty in power system adequacy," in *Proc. of IEEE 12th International Conference on Probabilistic Methods Applied to Power Systems (PMAPS2012)*, Istanbul, Turkey, june 2012, pp. 664–669.

[13] Energy Exemplar, "PLEXOS for Power Systems–Power Market Simulation and Analysis Software [computer software]," sep. 2012. URL http://www.energyexemplar.com/.

[14] B. Daniel, *Xpress-Optimizer Reference Manual*, Fair Isaac Corporation, Leamington Spa, Warwickshire, UK, Jun. 2009.

[15] Ministerio de Energía, Gobierno de Chile, "Campaña de Prospección Eólica en el Norte de Chile," Santiago, Chile, sep. 2010.

[16] J. R. McLean (Garrad Hassan and Partners Ltd.), "Equivalent wind power curves," Tech. Rep. for TradeWind Consortium, jul 2008.

[17] P. Nørgaard and H. Holttimen, "A multi-turbine power curve approach," in *Proceedings of Nordic Wind Power Conference NWPC'04*, Gothenburg, Sweden, mar. 2004.